American Journal of Nano Research and Application
2014; 2(6): 112-115
Published online December 19, 2014 (http://www.sciencepublishinggroup.com/j/nano)
doi: 10.11648/j.nano.20140206.11

Analysis of carbon nanotube device physics

Soheli Farhana*, Ahm Zahirul Alam, Sheroz Khan

Dept. of Electrical and Computer Engineering, International Islamic University Malaysia, 53100 Kuala Lumpur, Malaysia

Email address:
soheli.farhana@live.iium.edu.my (S. Farhana), zahirulalam@iium.edu.my (A. Zahirul), sheroz@iium.edu.my (S. Khan)

To cite this article:
Soheli Farhana, Ahm Zahirul Alam, Sheroz Khan. Analysis of Carbon Nanotube Device Physics. *American Journal of Nano Research and Application.* Vol. 2, No. 6, 2014, pp. 112-115. doi: 10.11648/j.nano.20140206.11

Abstract: In this paper, the device physics of carbon nanotubes is analyzed depend on the graphene structure. The analysis is done to calculate energy dispersion relation, effective mass and intrinsic carrier concentration of graphene to establish different carbon nanotubes. Diameters with different chiral vector (n, m) of carbon nanotubes vary the electronics properties of graphene. Different chiral vector of a graphene allows designing carbon nanotube (CNT) for different types of appliance, which can be achieved from the analyzed carrier concentration calculation. This investigation will helpful for further designing of CNT-based nano device.

Keywords: Carbon Nanotube, Graphene, Mass

1. Introduction

The mechanical properties as well as the electronics properties of carbon nanotubes made a drastic change in nano technology research to make it exceptional for researchers. Though carbon nanotubes are miniature tubes made of carbon atoms that are nanometer diameter and their length is larger and is about micrometers. Carbon nanotubes are made from rolled graphene into a test-tube shape [1] radius and covering angle of CNTs provide the electronic structure [2]. CMOS technology is going to be limited in terms of the dimension of electronics device which will be recovered by using CNTs [3]. Many applications have been proposed in earlier period researches for carbon nanotubes together with nano semiconductors devices [4-6]. Tight binding model of CNTs help to calculate the analytical solution of 1D graphene [7-10] figure out from the electronic structure.

2. Device Physics of CNT

The development of numerous next generations' device applications using CNTs are becoming to the researchers more attractive day by day for its exclusive electronic properties. In present research, researchers are very curious about the development of like field effect transistors or sensing elements by using CNTs. The wave vectors are quantized in the circumferential direction for the sake of very small radius of carbon nanotubes. Furthermore, the fineness of the nanotube's cylindrical shell obviously acquiesce an even smaller length of confinement in the radial direction, thus making the material virtually one-dimensional as far as electron transport is concerned [11-14].

2.1. Reciprocal Lattice

The primal cell of a CNT is described from the unit vectors by,

$$R_1 = \frac{a}{2}\left(\sqrt{3}\hat{x} + \hat{y}\right) \text{ and } R_2 = \frac{a}{2}\left(\sqrt{3}\hat{x} - \hat{y}\right) \quad (1)$$

where, R_1 and R_2 are the unit cell vectors of a CNT and a = 2.49 Å is the carbon to carbon atom distance between two carbon particles and reciprocal lattice vectors are:

$$a_1 = \frac{2\pi}{a}\left(\frac{1}{\sqrt{3}}\hat{x} + \hat{y}\right) \text{ and } b_1 = \frac{2\pi}{a}\left(\frac{1}{\sqrt{3}}\hat{x} - \hat{y}\right)$$

2.2. Graphene Electronic Structure

To examine the conductivity properties of the nanotube, a two dimensional graphene lattice is derived for calculating the energy dispersion for CNTs by,

$$E_{2D}(K) = \pm V_{pp\pi}\{3 + 2\cos(KR_1) + 2\cos(KR_2) + 2\cos[K(R_1 - R_2)]\}^{1/2} \quad (2)$$

where $V_{pp\pi}$ is the adjacent shift integral. The 3D view of graphene electronic structure is shown in Fig. 1.

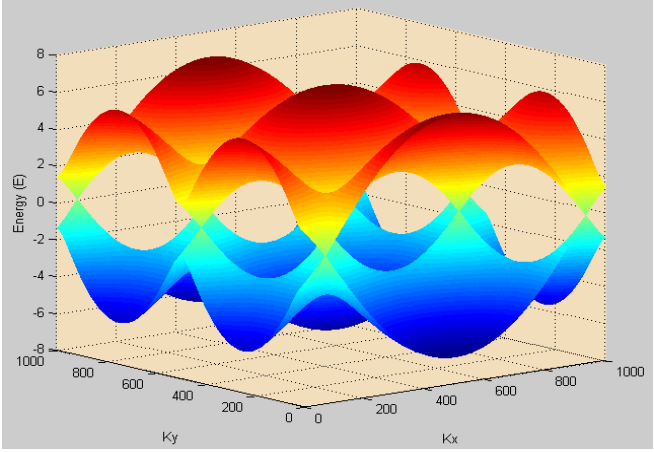

Figure 1. *Graphene electronic structure plot for valence and conduction band.*

A single-walled CNTs' 1D energy band can also be calculating by,

$$E_{1D}(k) = \pm V_{pp\pi}\left[1 + 4\cos\left(\frac{\sqrt{3}K_x}{2}a\right)\cos\left(\frac{K_y}{2}\right) + 4\cos^2\left(\frac{K_y}{2}\right)\right]^{1/2} \quad (3)$$

Here K_x and K_y are the wave vectors used in the equation (3)

$$(K_x, K_y) = \left(k\frac{K_2}{|K_2|} + qK_1\right) \text{ for } \left(-\frac{\pi}{|T|} < k < \frac{\pi}{|T|}, \text{and } q = 1, \ldots\ldots, N\right)$$

Here, k represents the wave vector and K_1 and K_2 represent the shared wave vectors beside the CNT axis, where the translational vector is denoted by $|T|$, and total hexagon unit cell is N. Therefore,

$$|T| = \frac{\sqrt{3}\pi d_t}{d_R} \text{ and } N = \frac{2(n^2 + nm + m^2)}{d_R}$$

Here d_R is GCD of $(2n + m)$ and $(2m + n)$. Therefore, K_1 and K_2 can be calculating by,

$$K_1 = \frac{(2n + m)b_1 + (2m + n)b_2}{Nd_R} \text{ and } K_2 = \frac{mb_1 - nb_2}{N}$$

2.3. Density of States

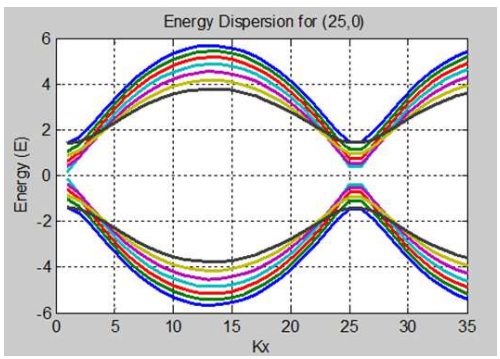

Figure 2. *Simulation of a CNT wave vectors in K-space with chiral vector of (25, 0).*

Vectors K_1 and K_2 dependent k-vectors (Figure 2) represent the single state area in momentum space $A_P^{1-state} = h^2|K_1||K_2|/2$ and a differential area as, $A_P = h^2|K_1|dk$, where dk is in the direction of K_2 and h is the Planck's constant. Therefore, per unit energy for the density of states is discussed follows,

$$D(E)dE = 2\frac{dA}{A_p^{1-State}} = \frac{4}{h^2|K_1||K_2|}h^2|K_1|\frac{dk}{dE} = \frac{2|T|}{\pi}\left(\frac{dE}{dk}\right)^{-1} \quad (4)$$

The density of states is simulated using equation (4) for the chiral vector of (25, 0) CNT is shown in Fig. 3.

Density of states (DOS) calculation involves the custom of numerical method due to the difficulty and association of the instances. Thus the energy dispersion relation designed in extract equation for the 1D DOS is as follows,

$$D(E)dE = \sum_i^{AllBand}\frac{4}{\pi V_{pp\pi}a\sqrt{3}}\frac{E}{\sqrt{E^2 - E_{c\,min_i}^2}}dE \quad (5)$$

where E_{cmin} is the transmission least value for the selected band. This least value is simulated in the following Fig. 2. DOS is recalculated from (5), the approximated simulation of DOS is shown in Fig. 3.

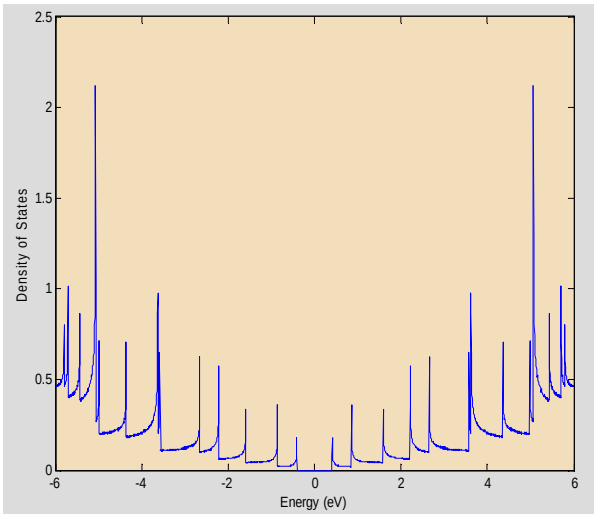

Figure 3. *CNT (25, 0) DOS simulation which accumulate the approximate.*

2.4. Effective Mass

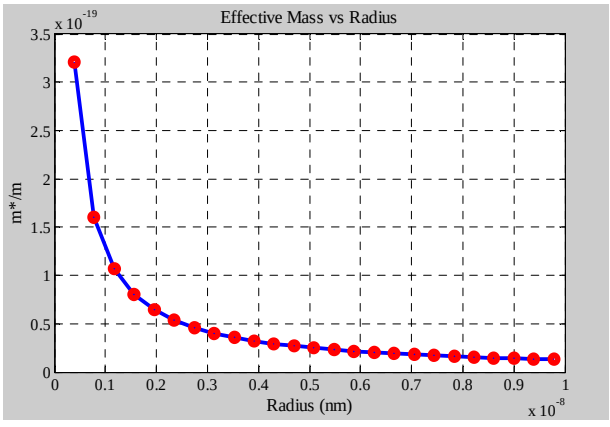

Figure 4. *Simulation of the various chiral vector (n,m) electrons.*

Effective mass for a single band can be analyzed from (3) and it can be represent the absolute explanation for the CNT energy dispersion. The effective mass calculation for a semiconductor is defined in (6),

$$m_i^* = \frac{h^2}{\left(\frac{d^2E}{dk^2}\right)} \quad (6)$$

Equation (6) is designed further for the various CNT's with chiral vector of (n,m) electron effective mass is simulated shown in Fig. 4.

Equation (6) represents the analysis of the effective masses of CNT which differ with the chiral vector extolled in (n, m) index.

2.5. Intrinsic Carrier Concentration

The carrier concentration of CNTs can be considered from the DOS. Semiconductors carrier concentration is represented by,

$$n_{cnt} = \int_{E_c}^{\infty} D(E)f(E)dE \quad (7)$$

Here DOS is denoted by D(E), Fermi level is denoted by f(E), and Conduction band minima is denoted by E.

Carrier concentration can be found from (5),

$$n_{cnt} = \sum_i^{All\ Bands}\left[\frac{4}{\pi V_{pp\pi}a\sqrt{3}}\cdot\int_{E_c}^{\infty} E(E^2 - E_{Cmin_i}^2)^{-1/2} + \left(1 + e^{\frac{E-E_F}{KT}}\right)^{-1} dE\right] \quad (8)$$

$$n_{cnt} = \frac{4}{\pi V_{pp\pi}a\sqrt{3}}\int_0^{\infty}(E' + E_c)(E^2 + 2E_cE')^{-1/2}\left(1 + e^{\frac{E'-E_F+E_c}{KT}}\right)^{-1} dE' \quad (9)$$

In addition, insignificant transmission least value causes the dropped at the Fermi function ahead of the first band.

Let x = E/KT and $\eta = \frac{E_F - E_c}{KT}$, to solve the difficulties from (9),

$$n_{cnt} = \frac{4\sqrt{KT}}{\pi V_{pp\pi}a\sqrt{3}}\int_0^{\infty}(KTx + E_c)[x(KTx + 2E_c)]^{-1/2}(1 + e^{x-n})^{-1}dx \quad (10)$$

Two efficient restrictions is formulated in this work using the Fermi integral,

L1: $\eta \ll -1$

$$n_{cnt} = N_c I e^{\frac{E_F - E_c}{KT}}$$

L2: $\eta \gg 1$, $n_{cnt} = N_c \frac{(E_F^2 - E_c^2)^{1/2}}{KT}$

where $N_c = \frac{4\sqrt{KT}}{KT}$ and, $I\sqrt{\frac{E_c}{2KT}}\frac{1}{\sqrt{KT}}\int_0^{\frac{6R_c}{KT}}\frac{(KT\,x + E_c)}{x^{1/2}(KT\,x + 2E_c)^{1/2}}e^{-x}dx$

Numerical integration method can be calculated this integral [26]. The higher boundary is substituted from infinity to $\frac{6R_c}{KT}$, zero can be neglected as for values beyond this limit. The inferior limit is changed to 0+, at x = 0 to be $\frac{E_c}{2KT}$.

Carrier concentration is simulated for different CNTs (n,m) chiral vectors is shown in Fig. 5.

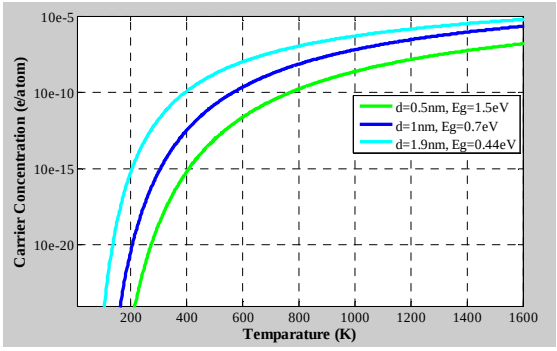

Figure 5. *Electron carrier concentrations for different carbon nanotubes.*

2.6. Doped Carbon Nanotubes

The ability to dope semiconducting materials is important for the realization of electronic devices. In nanotubes, doping can be accomplished in different ways: substitution of B or N atoms in the lattice, insertion of atoms inside of the nanotubes, electrostatically, and charge transfer from adsorbents or substrates. Here we are interested in establishing the basic equations that determine the position of the Fermi level in doped nanotubes. This can be accomplished with the help of the intrinsic carrier concentration with the doping fraction *f* (electrons/atom) can be expressed by the following equation,

$$f \approx \frac{9\sqrt{3}a^2 m^* \sqrt{E_g k_B T}}{4\pi^{3/2}h^2}\exp\left(\frac{E_F - E_c}{k_R T}\right) \quad (11)$$

The position of the Fermi level with respect to the conduction band edge become,

$$E_F - E_c = k_B T \ln\left(\frac{2\pi^{3/2}\gamma^{1/2}R^{3/2}f}{\sqrt{3}a^{3/2}g\sqrt{k_B T}}\right) \quad (12)$$

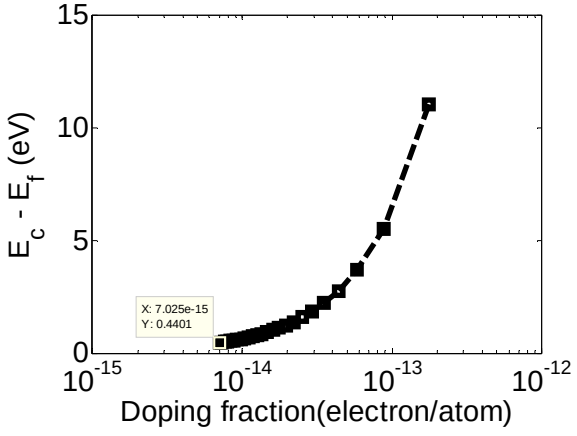

Figure 6. *Position of Fermi level with respect to the conduction band edge as a function of the doping fraction for the nanotubes with diameter of 1.95 nm.*

Thus Fig. 6 shows the behavior of this function at room temperature for nanotubes of different sizes, assuming a band degeneracy of one (for a doubly degenerate first band, the Fermi level is lower by $k_BT\ln 2$). Of note is the doping at which the Fermi level reaches the band edge, with a value of about 10^{-3} electrons/atom for nanotubes with radii in the 0.5~1 nm range. In fact, this doping is given by,

$$f^* = \frac{\sqrt{3}a^{3/2} g\sqrt{k_B T}}{2\pi^{3/2}\gamma^{1/2}R^{3/2}} = 5.2\times 10^{-3} g\frac{\sqrt{k_B T}}{R^{3/2}} \qquad (13)$$

where R is in nanometers and k_BT is in eV. At room temperature a good rule of thumb is $f^* \approx 10^{-3}/R^{3/2}$.

3. Conclusions

A brief explanation of CNT device physics is elucidated in this paper. The energy dispersion relation is explained and simulated using 2D graphene lattice in this research. Effective mass is analyzed for designing of optimum chiral vector design. Carrier concentration CNTs is drawn from the elaboration of density of states. This analysis will help the designer helps to construct in the electrical properties of carbon nanotubes as well as the conductivity of carbon nanotubes in the electronic band structure.

Acknowledgements

Authors would like to thank Ministry of Education, Malaysia through Fundamental Research Grant Scheme (FRGS).

References

[1] A. Jorio, A., Gene, D., and Mildred S. D., (2008). eds. Carbon nanotubes. advanced topics in the synthesis, structure, properties and applications. Vol. 111. Springer, 2008.

[2] M.J. O'connell, Sergei M. Bachilo, Chad B. Huffman,C.M. Valerie, S.S. Michael, H. Erik, Kristy, L. Rialon, (2002). Band gap fluorescence from individual single-walled carbon nanotubes. Science 297.5581 (2002): 593-596.

[3] A. Javey, J. Guo, Q. Wang, M. Lundstrom, H. Dai, (2003). Ballistic carbon nanotube field-effect transistors. Nature 424.6949 (2003): 654-657.

[4] P.A. Khomyakov, G. Giovannetti, P. C. Rusu, G. Brocks, J. Van den Brink, and P. J. Kelly, (2009). First-principles study of the interaction and charge transfer between graphene and metals. Physical Review B 79.19 (2009): 195425.

[5] F. Schwierz, (2008). Graphene transistors. Nature nanotechnology 5.7 (2010): 487-496.

[6] D.R. Paul, and L.M. Robeson L. M., (2008). Polymer nanotechnology: nanocomposites. Polymer 49.15 (2008): 3187-3204.

[7] W. Qiao, X. Li, H. Bai, H., Y. Zhu, Y. Huang, (2012). Structure and electronic properties of the nanopeapods—One dimensional polymer encapsulated in single-walled carbon nanotubes. *Journal of Solid State Chemistry*, *186*, 64-69

[8] Q. Cao, A.R. John, (2008). Ultrathin Films of Single-Walled Carbon Nanotubes for Electronics and Sensors: A Review of Fundamental and Applied Aspects. Advanced Materials 21.1 (2008): 29-53.

[9] J. C., Slater, (1974). Quantum theory of molecules and solids. New York: McGraw-Hill, Vol. 4.

[10] A.H. Neto, F. Castro, N.M. Guinea, R. Peres, S. Kostya, K. Andre, "The electronic properties of graphene." *Reviews of modern physics* 81, no. 1 (2009): 109.

[11] S. Farhana, A.Z. Alam, S. Khan and S. Motakabber,, (2013). Design and Development of a Simulator for Modelling Carbon Nanotube. Internatiiona Conference on Mechatronices (ICOM 2013), 2013, Kuala Lumpur, Malaysia

[12] S. Farhana, A.Z. Alam, S. Khan and S. Motakabber, (2013). Analysis of CNT Electronics Structure to Design CNTFET. Proceedings of the 5th IEEE International Nanoelectronics Conference, IEEE INEC 2013, 2-4 January, Singapore, pp. 352-354.

[13] S. Farhana, A.Z. Alam, S. Khan and S. Motakabber, (2013). Modeling of small Band-gap CNT for designing of faster switching CNTFET. Proceedings of the IEEE Business Engineering and Industrial Applications Colloquium 2013, Langkawi, Malaysia on 8 – 9 April 2013, pp. 565-568.

[14] S. Farhana, A.Z. Alam, S. Khan and S. Motakabber, (2013). Modeling of Optimum Chiral Carbon Nanotube using DFT. The 13th IEEE International Conference on Nanotechnology, Beijing, China, August 5th to 8th, 2013

[15] J. Zhang, A. Boyd, A. Tselev, M. Paranjape and P. Barbara, "Mechanism of NO2 detection in carbon nanotube field effect transistor chemical sensors", Appl. Phys. Lett., Vol. 88, p. 123112, 2006.

[16] R.J. Chen, H.C. Choi, S. Bangsaruntip, E. Yenilmez, X. Tang, Q. Wang, Y.-L. Chang and H. Dai, "Investigation of the mechanisms of electronic sensing of protein adsorption on carbon nanotube devices", J. Am. Chem. Soc., Vol. 126, p. 1563, 2004.

[17] W.E. Boyce and R.C. DiPrima, Elementary differential equations and boundary value problems, John Wiley and Sons, New York, 1986.

[18] S.M. Sze, Physics of semiconductor devices, John Wiley & Sons, New York, 1981.